A novel design for decoupling the energy storage and return in passive ankle foot prostheses: A redesign of the VSPA foot

Hashim A. Quraishi[1,2]

[1]Neurobionics Lab, University of Michigan, Ann Arbor, USA
[2]BioMechanical Engineering Department, Delft University of Technology, Delft, the Netherlands

***Abstract*— Conventional passive prosthetic feet cannot provide net positive mechanical energy, causing a strong reduction in push-off work. This decrease the comfortable walking speed and increases the metabolic cost of walking in amputees, as more than half of the positive work performed during able-bodied gait is done during the powered plantar flexion at the ankle joint. A possible contribution to enhance push-off is to utilize passive prostheses that can store and release energy by means of springs. This restores the push-off partially, enabling a higher self-selected walking speed and a lower metabolic cost**

Effective energy release at push-off is not just a matter of higher energy storage, but the release also needs to be well timed. Controlling the release rate of energy in current passive prosthetic feet is often constrained due to the unnatural ankle joint mechanics caused by simple spring behavior. The Variable Stiffness Prosthetic Ankle-Foot (VSPA-Foot) of Shepherd and Rouse (2017) tackles this problem by using a cam and follower transmission to decouple the leaf spring mechanics from the mechanics of the ankle joint. The cam profile determines the mechanics of the ankle joint, whereas the stiffness of the spring determines the energy stored for a particular deflection. Despite achieving this control of ankle mechanics, the VSPA still acts spring-like. This means that energy is stored and released in the exact same manner.

The purpose of this study was to decouple the energy storage and release characteristics. A prototype was build that uses two cam-profiles in order to do so. These cam profiles can differ in the way they store and release energy, as long as the total energy stored or released is at most equal (thereby not violating the laws of thermodynamics). By using multiple cam profiles, energy can be stored in the initial part of the stance phase. Rather than returning this energy instantaneously, it is released during late stance to enhance the push-off. This is a continuous approach to the energy recycling concept originally proposed by Collins and Kuo (2010).

Implementing the energy recycling concept in the VSPA foot redesign removed the hysteresis losses found whilst using a single cam profile and showed net positive work done during the push-off phase.

I. Introduction

Transtibial amputations account for more than 25% of dysvascular limb-loss discharges in the United States [1]. Due to the aging population, the number of Americans living with lower limb amputations is expected to keep on increasing [2]. The loss of a lower limb has significant effect on gait, as the human ankle is responsible for the majority of positive work done during gait [3] (as described by [4]). Therefore, the lack of ankle musculature can cause a strong reduction in push-off work, which is often compensated by other joints. This can lead to greater joint stresses which in turn can cause long term health issues and co-morbidities due to asymmetrical joint loadings [5]. Enhancing the push-off at the ankle joint in active prostheses can reduce these issues, decrease the metabolic cost [6], increase the self selected walking speed [6][7] and increase user satisfaction [8].

Energy storage and return (ESR) feet are passive prosthetic feet used to partially restore the push-off by returning mechanical energy in the late stance that was stored during the controlled dorsiflexion in mid-stance. The effectiveness of the push-off, however, does not depend on the mere quantity of energy release, but also its release rate. This has already been investigated for exoskeletons [9][4]. Furthermore, walking models have shown that the collision losses of the leading intact leg during the step-to-step transition can be reduced by increasing the push-off of the trailing leg [10].

The aim of this study was to design a Decoupled Energy Storage and Return (DESR) ankle foot prosthesis. It should have the ability to modulate the ankle mechanics independent of the elastic element in the system. The device should also allow the energy to be stored in a different manner than it is released, as long as the energy stored and released are at most equal. A potential benefit of this concept would be to store energy in the early stance phase and transfer this to the late stance phase in order to enhance the push-off as illustrated in figure 1, where a positive angle represents dorsiflexion and a negative angle represents plantar flexion. From this point on the blue curve and/or cam profile will reference to the blue curve in figure 1b and the red curve and/or cam profile will reference to the red curve in figure 1b.

II. Concept

A. VSPA foot

The design of the VSPA-Foot of Shepherd and Rouse (2017) [11] is a key aspect of our new mechanism. The primary goal of the VSPA foot was to enable the production of non-linear torque angle curves, in order to reproduce the able-bodied torque-angle curve during level-ground walking as closely as possible. The torque-angle curve for the VSPA foot was designed using the kinetics and kinematics data of Bovi et al. as a reference for the human joint capabilities [12]. Figure 2 from Shepherd (2017) [11] displays the torque angle curves for normal walking, stair descent [12] and for standing upright [13]. These values are estimated for a 70

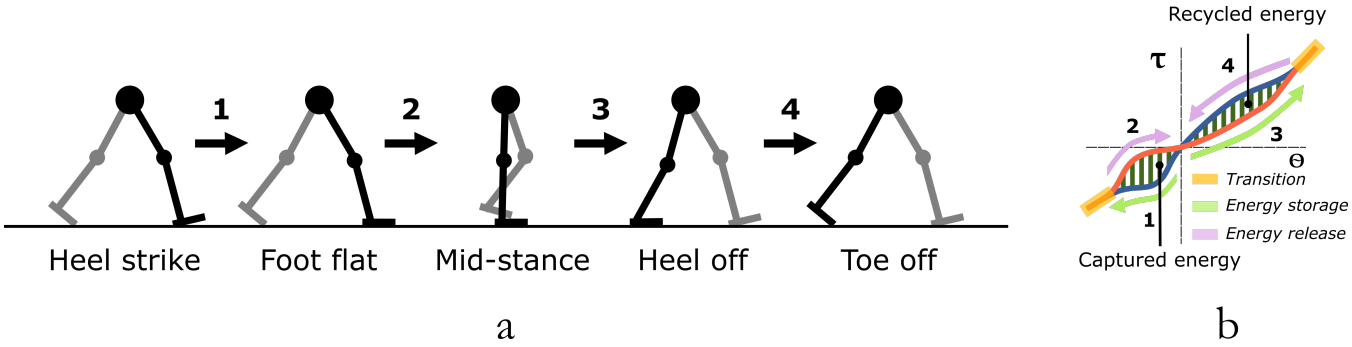

a b

Fig. 1: (a) Key positions in the stance phase. (b) The DESR ankle joint response torque plotted over the ankle angle throughout gait, along the same key positions as mentioned in part 'a' of this figure. This illustrates that energy captured early in the stance phase, can be recycled to enhance the push-off during late stance. Here a positive angle represents dorsiflexion and a negative angle represents plantar flexion.

kg subject. The gray lines during 'Normal Walking' in figure 2 illustrate the push-off in level ground walking, where the biological ankle performs net-positive mechanical work. This push-off cannot be reproduced by a (quasi-)passive prosthesis due to its inability to generate energy. Here the term 'quasi' indicates the presence of an actuator in the prosthesis. This actuator, however, is merely used to change the properties of the prosthesis and does not inject energy into the gait cycle. Due to the lack of energy generation, the VSPA foot tries to replicate the human ankle during the "controlled plantar flexion" and "controlled dorsiflexion" phase, where the human ankle functionalities can be reproduced with a quadratic/non-linear spring.

Performing different ambulatory tasks requires a change in quasi-stiffness of the ankle, as can be seen in figure 2. The quasi-stiffness and stiffness are the same for passive prostheses. For a more extensive explanation about the difference between the two, see [14]. The VSPA foot allows for a variablity in stiffness by using a 10 W DC motor with a 3,9:1 planetary gearhead (DCX 16L, Maxon Motors, CHE). The redesigned prosthesis uses the same motor as the VSPA, which is illustrated in figure 3, along with the rest of the DESR components. Figure 4 shows the two key design elements of the VSPA. On the left is the cam-follower transmission that decouples the ankle joint mechanics from the leaf spring mechanics, allowing for non-linear and arbitrary torque angle curves. On the right is the stiffness variability component, where the stiffness of the spring can be adjusted by moving the slider support underneath the spring by using a motor.

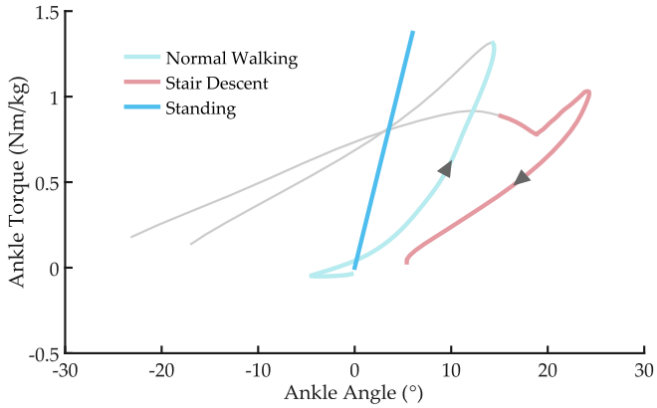

Fig. 2: Torque-angle curves for able-bodied subjects for various ambulatory tasks throughout the stance phase. For normal walking the blue part of the curve illustrates heel strike to push-off. For stair descent the red part of the curve illustrates heel strike to toe-off (from [12]). These values are estimated for a 70 kg subject. The gray parts of the curve require energy generation by the muscles and cannot be reproduced using a quasi-passive prosthesis. An estimate of the ankle stiffness is also plotted for quiet standing, for a 70 kg subject as well [13]. (figure Reprinted from Shepherd, 2017[11].

B. DESR foot

The primary goal of the DESR foot is to redesign the VSPA foot [11] in such a way that the energy storage and release characteristics of this prosthesis can be decoupled. The DESR foot is designed by examining the torque-angle relationship of the ankle throughout gait, rather than the power and timing relationship.

One of the possible benefits of decoupling the energy storage and return could be the ability to use energy stored in early stance to enhance the push-off in late stance in order to help propel the body forward (Fig 1). The general energy recycling concept was previously proposed by Collins & Kuo (2010) [15] with their Controlled Energy Storage and Return (CESR) prosthetic foot. They used a clutch based mechanism to timely store and release the captured energy in order to enhance the push-off. Testing the CESR foot with amputees showed an increased push-off at the prosthetic limb, however, this did not result in a reduced metabolic rate. Subjective metrics such as comfort were not mentioned [16]. A reason for the lack of metabolic rate reduction could be due to additional muscle work performed to control the energy release. Using a gradually controlled energy release method, such as the VSPA-foot cam-based transmission, rather than a clutch based mechanism might decrease this additional work done by the muscles.

This paper will mainly discuss the merging process of the cam-based transmission of the VSPA foot with the energy recycling concept of the CESR foot. This requires the use of

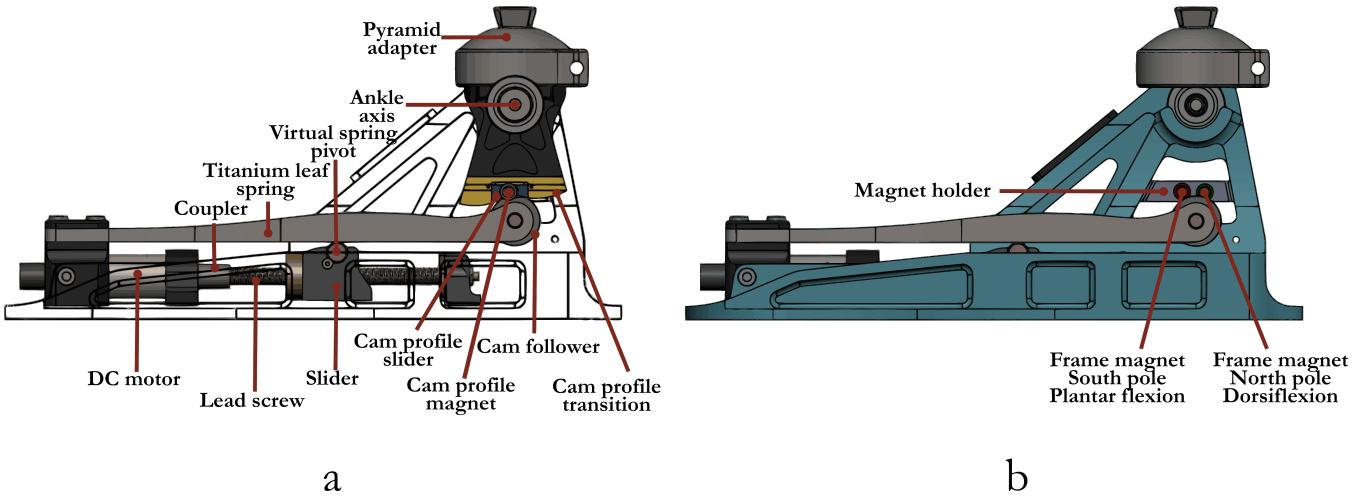

Fig. 3: (a) Key internal components of the DESR foot highlighted. (b) The magnet holder in the frame along with the frame magnets that cause the automatic switching between cam profiles are highlighted.

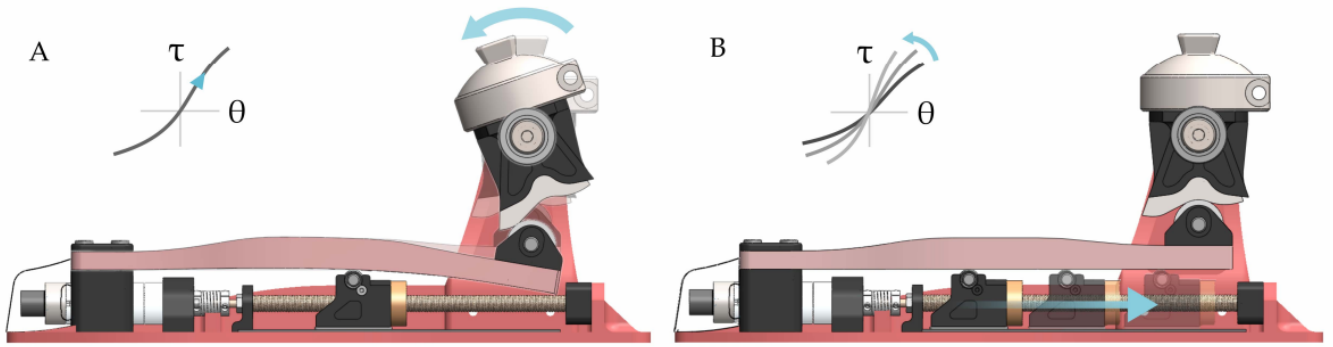

Fig. 4: (A) An angular deflection of the ankle center of rotation axis causes the spring to deflect around the virtual spring pivot point. The contact between the cam profile and cam follower causes this deflection. The cam profile can theoretically be shaped to achieve any arbitrary torque angle curve. The virtual spring pivot point around which the cam profile is shaped is called the "primary slider position" and the torque angle curve at this position is the "primary torque angle curve". (b) The motor below the spring can move the pivot point in the fore-aft direction in order to modify the rotational stiffness of the spring. The cam profile shape is fixed, but changing the spring stiffness can act as an amplification factor along the primary torque angle curve, making the ankle joint stiffness more or less stiff than at the primary position (Reprinted from Shepherd (2017) [11])

two separate torque-angle curves and thus two separate cam profiles. In order to apply the energy recycling concept by modulating different torque angle curves, the energy should be stored in a different manner than it is released. Figure 1 shows what this would look like in the torque angle plane throughout the stance phase.

Energy recycling can be applied in the DESR foot by introducing the ability to switch between torque angle curves. The use of multiple curves, and thus multiple cam profiles, eliminates the instantaneous energy return seen in clutch based mechanisms and provides the energy return in a controlled manner. After a certain amount of ankle flexion the two curves become identical in shape, marked as 'transition' in figure 1, allowing the ability to switch between curves. It is necessary for the response torque of both curves to be equal in order for the cam profiles to have identical shapes. The cam profiles should have identical shapes during the transition in order to have a smooth switch between cam profiles and to prevent any energy losses.

Though the variability of spring stiffness can prove to be useful for performing tasks other than level ground walking or adapting to the personal stiffness preference of the amputees, it is optional to use in the DESR foot. This paper will mainly discuss the decoupled energy storage and return concept for a primary chosen stiffness value. The effects of varying stiffness values on the energy recycling will be briefly discussed.

III. Design

A. Mechanical description

1) Order of engagement: The DESR foot combines the cam-based transmission and stiffness variability of the VSPA foot with the energy recycling concept of the CESR foot. The passive nature of the device does not allow for the generation of net external mechanical energy. Therefore, the two torque angle curves can differ in shapes, as long as the total area energy released does not exceed the energy stored in the system. If we look at the order of engagement in figure 1, it is clear that the total area under the blue and red curves is not equal. The reason behind this is that the curves are not

classified by their energy storage capabilities, but rather the action they perform during gait. It is clear that the red curve is only engaged during a dorsiflexion movement, whether it is towards or away from the equilibrium angle of zero degrees, and thus storing or releasing energy. The blue curve is only engaged during a plantar flexion motion. The correct order of engagement of these curves is essential in order to facilitate additional forward propulsion in the late stance.

The DESR foot has to transition between the curves after both the controlled plantar flexion and the controlled dorsiflexion in order for the energy recycling principle to enact during every stance phase of the prosthetic limb. In order to ensure this transitioning, amputee gait data of the VSPA-foot was used to determine the transitioning angles of 5 degrees at plantar flexion and 10 degrees at dorsiflexion [17].

2) Sliding cam profiles: The key component of the DESR foot is the dual cam-based transmission (Figure 5). In order to transition between torque angle curves, the cam profile is subdivided in a sliding part, where the the torque angle curves differ and the cam profiles differ in shape, and a transitioning zones, where both torque angle curves are equal and the cam profiles are identical in shape. If the cam follower, which is a simple roller bearing connected to the leaf spring (Figure 3), makes contact with the transitioning zone of the cam profile, the sliding part is under a no-load condition. This allows for a medio-lateral movement of the sliding part, ensuring a switch of engagement from one cam profile to the other. The medio-lateral movement occurs due to the presence of cleverly placed magnets. After controlled plantar flexion the magnets shift the cam profile slider such that a switch always occurs from the blue cam profile to the red cam profile, keeping in mind that similar poles of a magnet repel each other and opposite poles attract one another. Likewise, a switch from the red cam profile to the blue cam profile always occurs after controlled dorsiflexion. This is illustrated in figure 5, where the cam follower line of contact is indicated. The physical orientation of the cam profile is illustrated and the arrows 1-4 match the arrows drawn in the torque angle plane in figure 1. It should be noted that both cam profiles are identical in the transitioning zones, as the response torque for these is equal in the torque angle domain. As the switch of cam profiles after both the controlled plantar flexion and the controlled dorsiflexion can only occur in one direction, the arrows in figure 1 show the only possible order of engagement, assuming a switch between cam profiles always occurs. In case a switch between cam profiles does not occur, a single cam profile will stay engaged until the next stance phase of the prosthetic leg, where a switch can once again occur. This makes the system quite robust.

To permit, and ensure, the medio-lateral movement of the sliding part, a D9/h9 running fit tolerance was chosen in both the fore-aft and the vertical direction.

B. Customizable decoupled torque angle curves

The curves in the late stance phase were shaped around a linear torque angle relationship used by the VSPA foot amputee study as a reference, in order to stay within the human range of capabilities. It was reported by Shepherd et al. that the preferred stiffness values of the amputees were 341,1 to 811,4 Nm/rad [17]. The DESR stiffness values were designed with these preferred values in mind and has a stiffness range of 182,1 to 1221,6 Nm/rad during the controlled dorsiflexion. Whereas Shepherd et al. designed the plantar flexion slope to be 33% of the dorsiflexion slope, the DESR foot used a plantar flexion slope of 37% of the dorsiflexion to maximize the energy recycling capabilities. Since the torque values and the range of motion are much lower in the plantar flexion region, a steeper stiffness linear slope was chosen to increase the energy that can be potentially recycled.

Cubic spline interpolation was used to create the two torque angle curves that encompass the reference linear stiffness slope values from [17]. This might also prove useful in future studies to compare gait with a single cam profile versus a dual cam profile transmission.

C. Cam design

The stiffness of the leaf spring along with the shape of the cam profile, that causes the deflection of this spring throughout gait, determine the shape of the torque angle curve. The cam profile is manufactured for a primary chosen torque angle curve at a primary slider position of the virtual pivot point. Once the cam profile is machined, this primary torque angle curve is fixed. The ankle mechanics can still be adapted around this primary curve by changing the spring stiffness. This stiffness modulation will, however, act as an amplification factor along the whole primary torque angle curve, as illustrated in figure 4b. This section will discuss the mathematical relations in order to achieve a cam profile shape for a desired primary torque angle curve at a chosen primary slider position. Furthermore, the effects of adding a second cam profile will be discussed along with the adapted mathematical equations to determine the shape of this second cam profile.

A schematic overview of the geometric values are displayed in figure 6. Figure 6a shows the trigonometric relations for determining the blue cam profile and figure 6b shows the angular values that are different for the red curve. The blue and red curve are a reference to the red and blue torque angle curves in figure 1.

The principles of virtual work are applied here by considering this as a conservative energy system with no losses. In figure 6a the cam follower is modelled as a point, but the final cam profile curve will be offset by using the cam follower radius and applying the theorem of parallel curves. The rotation of the ankle joint θ results in a force between the cam profile and the cam follower. This generates a moment M_S around the spring, which is modelled as a rotary spring. For a rigid frame with infinite stiffness it can be assumed that the work stored into the spring, due to an angular deflection γ and moment M_S throughout the gait, should be equal to the work done at the ankle joint. However, experiments indicated some form of elastic deformation of the frame due to the response torque M_A around the ankle joint. This frame

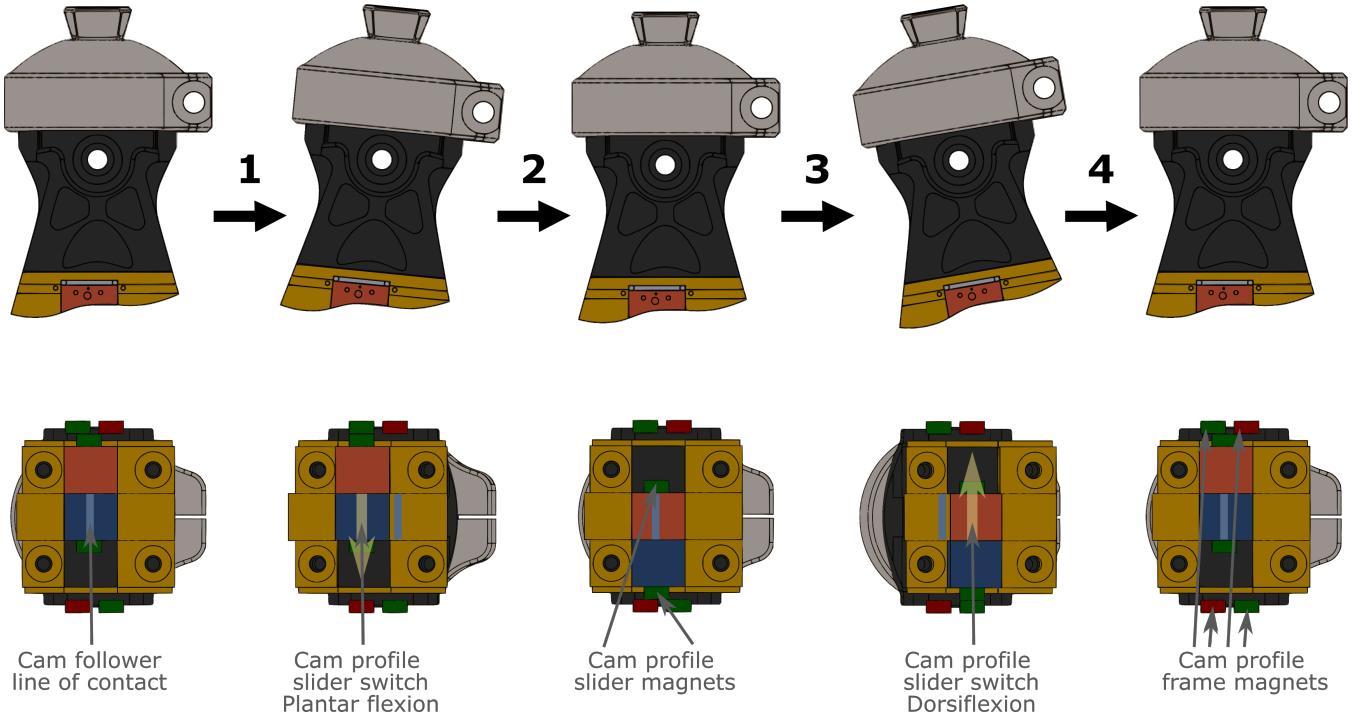

Fig. 5: The top part of the picture depicts the orientation of the cam profiles, relative to the neutral angle, throughout the gait cycle. The arrows correspond to the arrows and key positions during the stance phase mentioned in figure 1. The bottom of the figure shows the medio-lateral switch of the cam profiles. Transitioning between the two cam profiles, and thus the two torque angle curves, can occur when the cam follower line contact is in the 'transitioning zone', depicted with the yellow color. At that time the sliding part of the cam profiles is under a no load condition from the cam follower, and able to slide freely in the medio-lateral direction due to the magnetic forces acting on the sliding part. This switch occurs twice every stance phase, once when the transitioning plantar flexion angle is reached and once when the transitioning dorsiflexion angle is reached.

compliance δ, or elastic deformation of the frame, should be accounted for in the calculations. The mathematical model assumes a deflection δ of the frame proportional to the torque at the ankle joint. This stiffness was experimentally determined to be 2000Nm/rad. The relationship between the total energy stored in the ankle, the energy in the spring and the energy in the frame is defined by equation 1. The energy in the ankle minus the energy stored in the frame equals the energy stored in the spring:

$$\int_0^{\gamma} M_s d\gamma = \int_0^{\theta} M_A d\theta - \int_0^{\delta} M_A d\delta \tag{1}$$

where γ is the angular deflection of the rotary spring from the resting position, θ is the ankle angle, δ is the additional change in ankle angle due to frame compliance, and M_A and M_S are the respective torques around the ankle joint and the spring virtual pivot point. Here the M_S depends on the rotary stiffness 'k' of the spring, which can be converted from the experimentally determined translational stiffness values of the spring. This allows us to rewrite equation 1 into equation 2. In these equations the equilibrium position is at θ = 0° and dorsiflexion and plantar flexion are solved separately with 0 as the lower limit of integration.

$$\int_0^{\gamma} k(\gamma + \gamma_0) d\gamma = \int_0^{\theta} M_A d\theta - \int_0^{\delta} M_A d\delta \tag{2}$$

Integrating equation 2 provides the quadratic equation 3 which in turn can be solved using the boundary conditions that γ = 0 at θ = 0, giving us equation 4 as a result of the constant of integration c being zero.

$$\frac{1}{2}k\gamma^2 + k\gamma_0\gamma + c = \int_0^{\theta} M_A d\theta - \int_0^{\delta} M_A d\delta \tag{3}$$

$$\gamma(\theta) = -\gamma_0 + \sqrt{\gamma_0^2 + \frac{2}{k}\left(\int_0^{\theta} M_A d\theta - \int_0^{\delta} M_A d\delta\right)} \tag{4}$$

Besides the mechanical properties of the spring and frame, the final shape of the cam profile also depends on the geometrical constraints at the primary slider position. In order to solve for the final shape of the cam profile, the variables r and ψ have to be determined to achieve a polar representation of the cam profile. The radius r can be achieved by using the law of cosines, as seen in equation 5.

$$r(\theta) = \sqrt{L^2 + d^2 - 2Ld\ cos(\gamma + \sigma)} \tag{5}$$

The equation for ψ is

$$\psi(\theta) = \theta_{cam} - \alpha = \theta - \delta - \alpha \tag{6}$$

where α be derived by using the law of sines.

$$\alpha(\theta) = sin^{-1}(L\ sin(\sigma + \gamma(\theta))) - \omega \tag{7}$$

Here α is the deviation from vertical, caused by the horizontal displacement of the cam follower due the rotary motion the spring undergoes.

Equations 1-7 describe the modelling of the cam profile for the blue torque angle curve (Fig. 1). Modelling the cam profile from the red torque angle curve (Fig. 1) is similar, with slightly different boundary conditions. The key difference is that the red curve has energy stored at mid-stance, implying that the spring is bent at θ = 0 for the red curve. Figure 6b shows γ_{20} as an additional preload due to the energy stored between the two torque angle curves (see 'Captured energy' in figure 1). So the basic relationship between the energy stored in the ankle due to the spring and frame compliance for the red curve become can be described with equation 8. Note that the number '2' indicates the values of the red curve, e.g. γ_2 and σ_2.

$$\int_0^{\gamma_2} k(\gamma_2 + \gamma_0 + \gamma_{20}) d\gamma_2 = \int_0^{\theta} M_A d\theta - \int_0^{\delta_2} M_A d\delta_2 \quad (8)$$

Where γ_{20} can be found using equation 9.

$$\int_{\gamma_0}^{\gamma_{20}} kx\ dx = ES \quad (9)$$

Here ES is the energy captured between the curves, as illustrated in figure 1. Integrating equation 9 gives

$$\frac{1}{2}k\gamma_{20}^2 + c_{20} - [\frac{1}{2}k\gamma_0^2 + c_0] = ES \quad (10)$$

If γ_{20} = γ_0 is chosen as boundary condition, it is found c_{20} - c_0 = 0. This gives the additional pre-load γ_{20} illustrated in figure 6 due to the captured energy caused by a difference between the torque angle curve paths and can be calculated as follows

$$\gamma_{20} = \sqrt{\frac{2}{k}ES + \frac{1}{2}k\gamma_0^2} \quad (11)$$

Now that γ_{20} is known, equation 8 can be integrated to achieve equation 12. It should be noted that if the red and blue torque angle curves differ in shape, the frame compliance will be different as well.

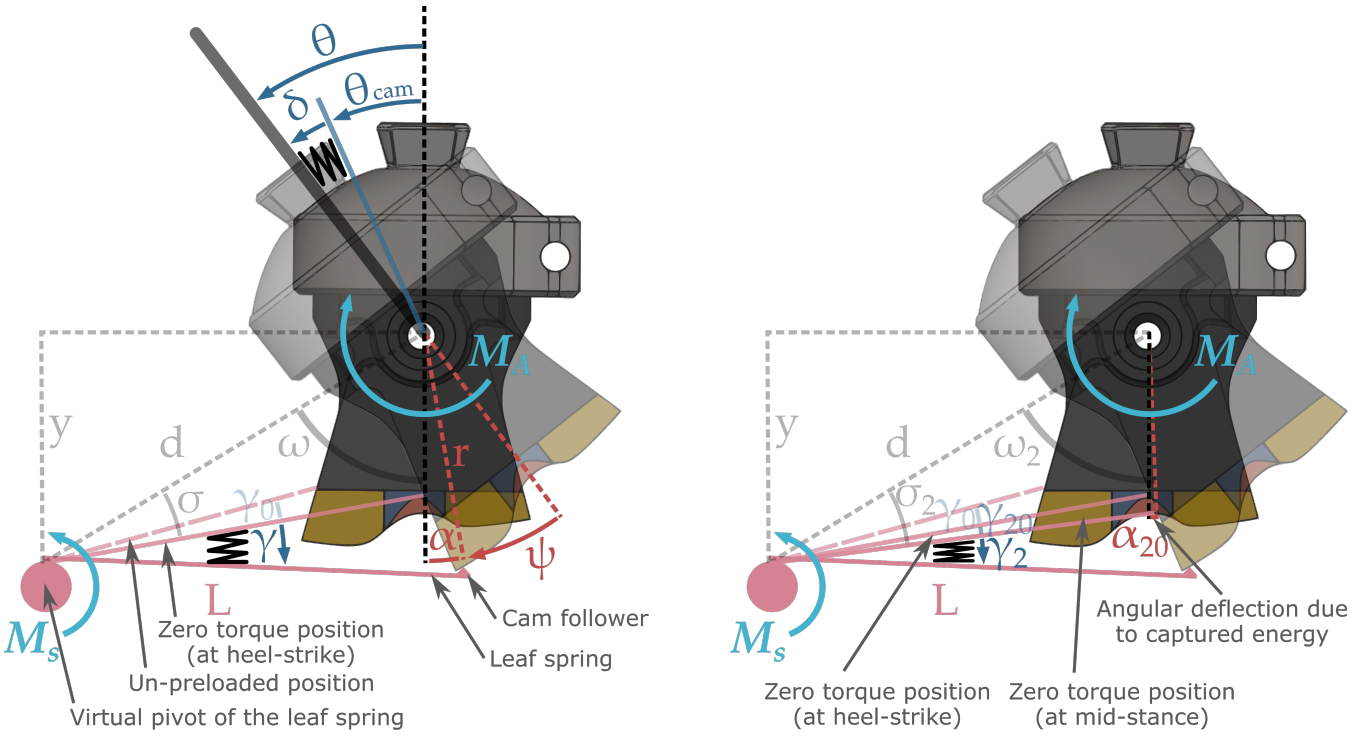

a b

Fig. 6: (a) The variables shown are used to determine the shape of the blue cam profile. Deflection of the spring, which is modelled as a linear rotational spring, around the virtual pivot point causes a response torque M_A at the ankle joint and an angular deflection θ of the ankle angle, causing the storage of work. The work stored in the ankle joint is equal to the work stored in the frame and the spring combined, where the frame compliance is noted as δ and the angular deflection of the ankle due to the cam deflection is noted as θ_{cam}. The value γ_0 is an initial pre-load of the spring in order to prevent backlash. The cam follower is modelled as a point for simplicity, but the actual cam profile will have an offset equal to the radius of the cam follower. The gray lines indicate the geometric variables to solve for the cam radius (r) using the angles γ, ψ and θ. (b) The second cam profile (red color) is designed in a similar manner as the blue one. The variable γ_{20}, however, is added as a pre-load to account for the energy capture in the system at mid-stance as illustrated in figure 1b. The addition of γ_{20} also changes the geometric angles shown in gray and adds a vertical deflection α_{20} at the equilibrium point. This is caused due to the spring motion not being purely vertical.

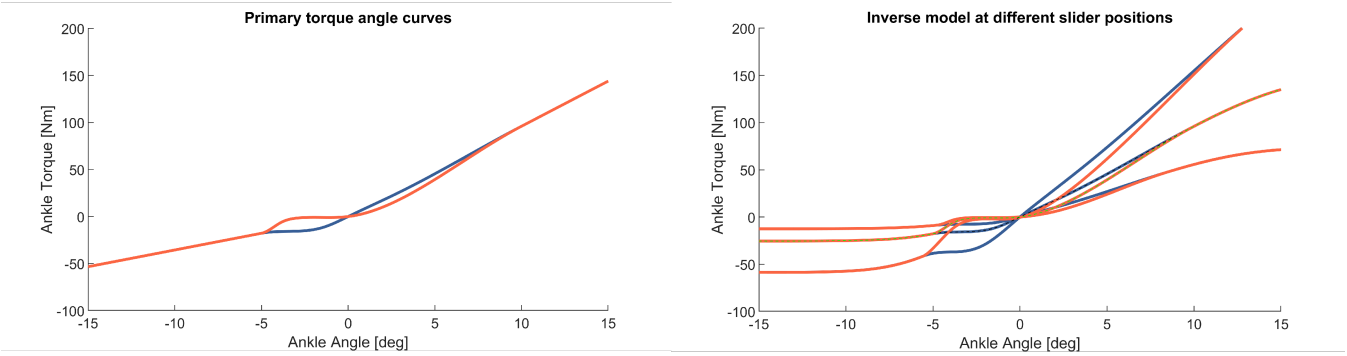

a b

Fig. 7: (a) The torque angle curves at the primary position of 34,4 mm are illustrated. The red and blue curve are shaped around a linear stiffness slope of 550,1Nm/rad. (b) The inverse model output is illustrated for the primary slider position and the positions 14,4 and 54,4 mm, where 54,4 mm is the stiffest setting.

$$\frac{1}{2}k\gamma_2^2 + k\gamma_0\gamma_{20}\gamma_2 + c = \int_0^{\theta} M_A d\theta - \int_0^{\delta_2} M_A d\delta_2 \quad (12)$$

Once again, c is found to be zero at θ = 0, as the main assumption is that all of the energy captured between the torque angle curves is stored in the spring. This is due to the prior assumption that the frame compliance is merely dependent on the ankle torque in order to simplify the math. Once again the quadratic equation can be solved

$$\gamma_2(\theta) = -(\gamma_0 + \gamma_{20}) + \sqrt{(\gamma_0 + \gamma_{20})^2 + \frac{2}{k}\left(\int_0^{\theta} M_A d\theta - \int_0^{\delta_2} M_A d\delta_2\right)} \quad (13)$$

The next step is to get the radius for the red cam profile using

$$r_2(\theta) = \sqrt{L^2 + d^2 - 2Ld\ cos(\gamma_2 + \sigma_2)} \quad (14)$$

where

$$\sigma_2 = \sigma + \gamma_{20} \quad (15)$$

The addition of γ_{20} to the red curve affects the values of σ_2, ω_2 and adds an angular deflection α_{20} of the ankle joint at the equilibrium angle as can be seen in figure 6b. To get the polar coordinates for the red cam profile, ψ has to be calculated once again by

$$\psi_2(\theta) = \theta_{cam2} - \alpha_2 = \theta_2 - \delta_2 - \alpha_2 \quad (16)$$

where

$$\alpha_2(\theta) = sin^{-1}(L\ sin(\sigma_2 + \gamma_2(\theta))) - \omega_2 \quad (17)$$

All the equations and calculations mentioned above are for determining the shape of the cam profiles for given torque angle curves

An inverse model is also created to predict the torque angle curves for machined cam profiles for slider positions other than the primary slider position. Not only does this allow the indication of the range of stiffness slope values, it also allows the prediction of the energy amount that can potentially be recycled. This inverse model accounts for the changes in the preload γ_0, the stiffness values of the spring and the change in trigonometric values such as 'd' and 'L' for changing the support slider position under the spring. An example of the output of this model is illustrated in figure 7. According to the inverse model, for a conservative system the energy in push-off, the area under the blue curve in the dorsiflexion region, should be between 9 and 10% higher compared to the energy stored under the red curve during dorsifelxion.

IV. Experimental Methods

The cam profile is designed for a primary slider position, but the support slider position can be moved in the fore-aft direction by a DC motor. The range of motion of the slider was 56 millimeters, with 0 being the most anterior position. The primary slider position was chosen at 34,4 millimeters to enable a large range of stiffness values. The actual slider position was determined using the motor encoder, whilst also accounting for the transmission ratio. It is important to use the most anterior hard stop as a homing position before starting the experiments.

The Joint Impedance Machine (JIM) at the Shirley Ryan Ability center was used to experimentally determine the actual torque angle curves of the DESR foot upon placing a moment at the ankle joint. The torque was sampled at 833,33Hz. The pyramid adapter of the DESR was rigidly attached to the JIM and the bottom of the foot was clamped down. The onboard ankle encoder data was resampled to plot against the torque values.

V. Results

The torque angle curves were determined for the blue cam profile without switching between cam profiles and also for both cam profiles with switching, to better map the effect of recycling energy. The experiments were performed for slider positions [4,4 ; 14,4 ; 24,4 ; 34,4]mm. By determining the torque angle curve of a single cam profile, the hysteresis

along this curve could be determined and taken into account for the dual cam profile set up. Table I shows the hysteresis values for plantar flexing (loading) and returning to the neutral angle (unloading) in early stance, as well as for dorsiflexing (loading) and returning to the neutral angle (unloading) in late stance. These hysteresis losses are likely caused by heat generation due to internal friction. Another possibility is the slight misalignment between the prosthesis ankle center of rotation and the JIM arm center of rotation. And finally, the losses could also be due to the clamps and bolts used to keep the prosthesis in place.

It appears that there are hysteresis losses in the dorsiflexion region of the torque angle curve, as the value is denoted to be negative. The energy recycling theorem is meant to decrease these losses and preferably have a positive value for the hysteresis dorsiflexion, meaning that more energy is released during push-off, than was stored in mid- to late stance.

TABLE I: Hysteresis single cam profile

Slider position (Single cam) mm	**Hysteresis plantar flexion** %	**Hysteresis dorsiflexion** %
4,4	-4,47	-4.06
14,4	-11,86	-4.08
24,4	-11,77	-4.48
34,4	-8.90	-3.17

Table 2 shows that a positive hysteresis is achieved with the dual cam based transmission of the DESR. These values are, however, lower than the expected 9% increase. The captured energy is between 5,38 and 6,41 %, implying that more work could be done during push-off than with a conventional prosthesis. However, after accounting for losses, the increase of push-off ends up between 1,01 and 2,44%. The torque angle curves for the single and dual cam profile experimental values at the primary stiffness setting are plotted in figure 8. Another interesting note was that the neutral position ,where the torque is zero in the torque angle plane, of the red torque angle curve became more plantar flexed with an increasing stiffness values. By plantar flexing the neutral ankle angle at mid-stance, the range of motion for energy storage can be increased. Data should be collected from multiple sets of cam profiles for a better understanding of the ankle behavior in the torque angle plane whilst using a dual cam based transmission.

TABLE II: Hysteresis dual cam profile

Slider position (Dual cam) mm	**Energy captured** %	**Hysteresis dorsiflexion** %	**Efficiency** %
4,4	5,38	1,01	18,79
14,4	5,73	1,46	25,47
24,4	6,16	1,44	23,39
34,4	6,41	2,44	34,97

VI. Discussion

The paper discussed the theoretical concept behind the DESR foot, the design requirements, hardware realization and the validation of the device. The main goal was to use energy from early stance to enhance the push-off in late stance.The characterization indicated that a 'figure eight' trend for energy recycling was apparent, but not to a full extent. Figure 8b shows that the actual energy captured is less than the desired energy. Testing a second pair of cam profiles could help describing this discrepancy. It could also be caused by the simplified assumption of torque dependent proportional frame compliance. The cam profiles were tested up to 34,4 mm, which is the primary slider position. The first set of cam profiles were not hardened to ease the post-machinability of parts. As the parts were not hardened, higher stiffness values were avoided during the prilimenary tests to prevent plastic deformation of any kind. Unfortunately, the sliding part of the cam profile was delivered in two separate pieces, which required a lot of post machining. This could be yet another reason for the discrepancy between the desired and experimental torque angle curves.

This paper only discussed one of the potential benefits of decoupling the energy storage and release in passive prosthesis. The DESR foot allows for the ability to test new concepts with passive prostheses that were not possible

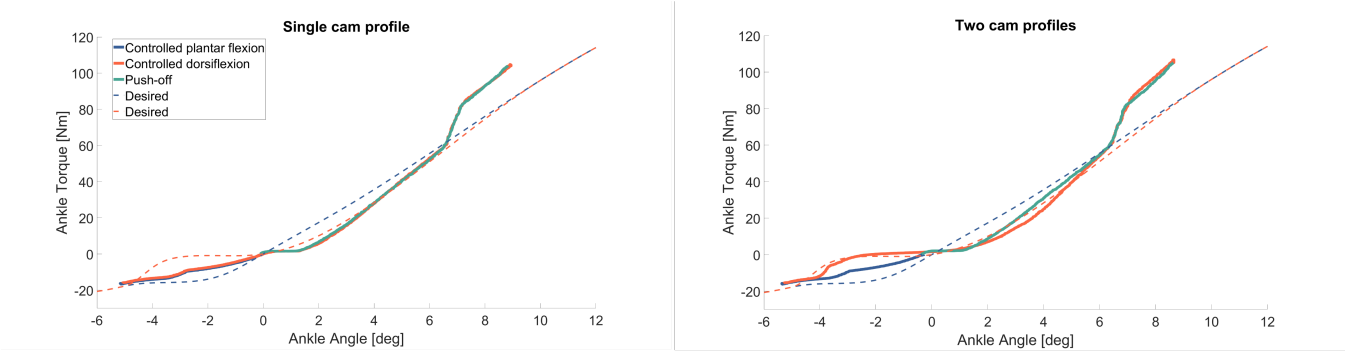

a b

Fig. 8: (a) A single cam profile undergoes a loading and unloading cycle in plantar flexion and dorsiflexion to determine the hysteresis losses of the system. (b) The torque angle curves for using two cam profiles are plotted, under the same experimental conditions as part 'a' of this figure. It is clear that a 'figure eight' shape is apparent

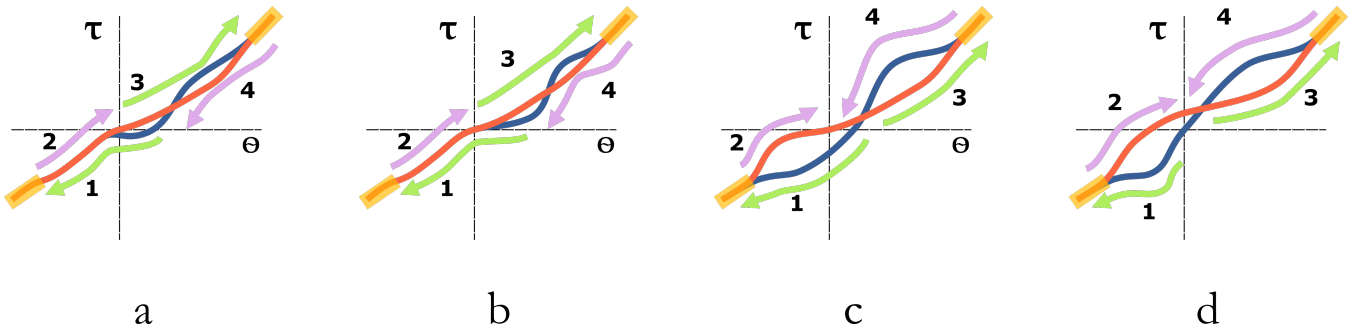

Fig. 9: (a) Alternative uses for decoupling the energy storage and release. The blue curve could have an initially dorsiflexed neutral ankle angle to prevent toe scuffing during gait. The shape of the blue and red cam profile would differ slightly in the mid- late stance, to compensate for the slight difference in neutral ankle angles. This is necessary, as the total amount of area under both curves has to be equal. (b) The release rate of energy could be separated for dorsiflexion and plantar flexion in the late stance. This could provide more insight about whether the optimal rate of energy storage and release should be equal or not. (c) This is a combination of the concept mentioned in part 'a' of this figure and the energy recycling concept. Combining the two concepts allows for foot clearance during the swing phase, whilst simultaneously increasing the range of motion along which energy can be 'captured'. (d) The neutral angle of the red curve is plantar flexed slightly to increase the range of motion for capturing energy. This, however, seemed to already appear to some extent in the gathered experimental data.

before. Figure 9 illustrates a couple of the concepts in the torque angle plane. The arrows once again indicate the same key positions during the stance phase of the gait as illustrated in figure 1. In these figures arrow 1 always indicates the controlled plantar flexion along the blue curve. Arrows 2 and 3 indicate the controlled dorsiflexion along the red curve. Finally, arrow 4 always indicates push-off along the blue curve. In all the torque angle curves illustrated, the absolute area under arrows 1 and 3 combined should be equal to the absolute area under arrows 2 and 4, implying that the energy stored in the system is at most equal to the energy released.

The first alternative concept in figure 9a illustrates that the foot is dorsiflexed in its unloaded position during swing phase, meaning the zero-torque position is at a dorsiflexed angle. This could potentially help the prevention of toe scuffing during gait and decrease the compensatory knee flexion to achieve toe clearance [18].

The second alternative in figure 9b shows a difference in the storage and release rate of energy in mid-stance to late stance. It is unknown whether this concept provides any additional benefits compared to conventional prostheses, but it would allow for investigating, and potentially optimizing, the energy storage and release independent of each other.

The third alternative in figure 9c combines the energy recycling concept with the first alternative mentioned above. A dorsiflexed neutral position of the blue curve would potentially prevent toe scuffing, whilst also applying the energy recycling concept in order to enhance the push-off. Due to the dorsiflexed neutral position, the range of motion for capturing energy during controlled plantar flexion also increases. Or the energy could be stored over the same range of motion with a smaller transitioning angle at controlled plantar flexion. This is beneficial to ensure the switch between cam profiles, as the transitioning angle after controlled plantar flexion is considerably lower than the transitioning angle after controlled dorsiflexion.

The fourth and final alternative in figure 9d moves the zero-torque point of the red curve in the plantar flexed region. The energy recycling concept is applied here once again, and the adjustment of the red curve increases the range of motion for capturing energy to potentially increase the push-off more than with the standard energy recycling concept discussed in the paper. This concept seemed to naturally occur during the experimentation. It is most likely due to the simplified assumptions of the frame compliance merely depending on the torque.

All the above-mentioned alternatives assume two transitions between the torque angle curves during each stance phase. The switching mechanism could also be designed such that it does not automatically switch between cam profiles, but that it is done on command or by intent recognition. The first alternative from figure 9a for instance could still have two cam profiles side-by-side. However, the red torque angle curve could be designed for level ground walking, and the blue torque angle curve would be used during e.g. stairs and ramp ascent, where a dorsiflexed neutral ankle angle could decrease the compensatory gait by other joints. The switch between cam profiles should then be achieved during the last step of level ground walking to ensure that the blue cam profile is engaged before the stair ascent.

Further work for the energy recycling concept requires testing with amputees in order to determine the clinical relevance of the concept. Afterwards, the optimal transitioning angles, stiffness slopes and amount of energy recycling can be determined. The possible benefits of the alternative concepts should also be assessed along with the feasibility of developing a physical prototype.

VII. Conclusion

This paper proposed a new concept to decouple the energy storage and release in passive ankle-foot prostheses. The VSPA foot was redesigned to use its cam based transmission. To physically realize this concept, two non-linear torque-angle curves were used to design a dual cam-follower transmission. The ankle range of motion and amputee preferred stiffness value range from a VSPA-foot study were used as

design requirements. A testing rig was used to determine the accuracy of the mathematical model by comparing the desired torque-angle curves with the experimentally achieved values. Future work will involve the investigation of the other possible benefits of energy storage and release decoupling, along with gaining a better general understanding of how the ankle behavior is influenced by using multiple cam profiles. Clinical tests will have to be performed to determine optimal transitioning angles and better understand the effects of energy recycling on amputee gait.

ACKNOWLEDGMENT

First of all the author would like to thank his daily supervisor Elliott J. Rouse for being the project sponsor and providing guidance throughout the whole project. Max K. Shepherd, being the designer of the original VSPA foot, provided feedback on the mechanical and conceptual design throughout the project and helped with acquiring the testing data from the JIM. Furthermore, the chairman of the thesis committee Dick H. Plettenburg gave his insights on mechanical design aspects, provided feedback on the progress of the project and helped streamlining the contact between the University of Michigan and the Delft University of Technology. The thesis supervisor Jaap Harlaar helped with understanding the clinical relevance of the DESR foot by providing his knowledge of biomechanics. He also gave feedback on the writing and interim presentations. Lastly the author would like to thank his friends and family for their support throughout the project.

REFERENCES

[1] T. R. Dillingham, L. E. Pezzin, and E. J. MacKenzie, "Limb amputation and limb deficiency: epidemiology and recent trends in the united states," *Southern medical journal*, vol. 95, no. 8, pp. 875–884, 2002.

[2] K. Ziegler-Graham, E. J. MacKenzie, P. L. Ephraim, T. G. Travison, and R. Brookmeyer, "Estimating the prevalence of limb loss in the united states: 2005 to 2050," *Archives of physical medicine and rehabilitation*, vol. 89, no. 3, pp. 422–429, 2008.

[3] D. Winter, "The biomechanics and motor control of human gait. waterloo," 1987.

[4] P. Malcolm, W. Derave, S. Galle, and D. De Clercq, "A simple exoskeleton that assists plantarflexion can reduce the metabolic cost of human walking," *PloS one*, vol. 8, no. 2, p. e56137, 2013.

[5] L. Nolan and A. Lees, "The functional demands on the intact limb during walking for active trans-femoral and trans-tibial amputees," *Prosthetics and orthotics international*, vol. 24, no. 2, pp. 117–125, 2000.

[6] H. M. Herr and A. M. Grabowski, "Bionic ankle–foot prosthesis normalizes walking gait for persons with leg amputation," in *Proc. R. Soc. B*, vol. 279, pp. 457–464, The Royal Society, 2012.

[7] A. R. De Asha, L. Johnson, R. Munjal, J. Kulkarni, and J. G. Buckley, "Attenuation of centre-of-pressure trajectory fluctuations under the prosthetic foot when using an articulating hydraulic ankle attachment compared to fixed attachment," *Clinical Biomechanics*, vol. 28, no. 2, pp. 218–224, 2013.

[8] R. E. Quesada, J. M. Caputo, and S. H. Collins, "Increasing ankle push-off work with a powered prosthesis does not necessarily reduce metabolic rate for transtibial amputees," *Journal of biomechanics*, vol. 49, no. 14, pp. 3452–3459, 2016.

[9] S. Galle, P. Malcolm, S. H. Collins, and D. De Clercq, "Reducing the metabolic cost of walking with an ankle exoskeleton: interaction between actuation timing and power," *Journal of neuroengineering and rehabilitation*, vol. 14, no. 1, p. 35, 2017.

[10] J. M. Donelan, R. Kram, and A. D. Kuo, "Simultaneous positive and negative external mechanical work in human walking," *Journal of biomechanics*, vol. 35, no. 1, pp. 117–124, 2002.

[11] M. K. Shepherd and E. J. Rouse, "The vspa foot: A quasi-passive ankle-foot prosthesis with continuously variable stiffness," *IEEE Transactions on Neural Systems and Rehabilitation Engineering*, vol. 25, no. 12, pp. 2375–2386, 2017.

[12] G. Bovi, M. Rabuffetti, P. Mazzoleni, and M. Ferrarin, "A multiple-task gait analysis approach: kinematic, kinetic and emg reference data for healthy young and adult subjects," *Gait & posture*, vol. 33, no. 1, pp. 6–13, 2011.

[13] P. G. Morasso and M. Schieppati, "Can muscle stiffness alone stabilize upright standing?," *Journal of neurophysiology*, vol. 82, no. 3, pp. 1622–1626, 1999.

[14] E. J. Rouse, R. D. Gregg, L. J. Hargrove, and J. W. Sensinger, "The difference between stiffness and quasi-stiffness in the context of biomechanical modeling," *IEEE Transactions on Biomedical Engineering*, vol. 60, no. 2, pp. 562–568, 2013.

[15] S. H. Collins and A. D. Kuo, "Recycling energy to restore impaired ankle function during human walking," *PLoS one*, vol. 5, no. 2, p. e9307, 2010.

[16] A. D. Segal, K. E. Zelik, G. K. Klute, D. C. Morgenroth, M. E. Hahn, M. S. Orendurff, P. G. Adamczyk, S. H. Collins, A. D. Kuo, and J. M. Czerniecki, "The effects of a controlled energy storage and return prototype prosthetic foot on transtibial amputee ambulation," *Human movement science*, vol. 31, no. 4, pp. 918–931, 2012.

[17] M. K. Shepherd, A. F. Azocar, M. J. Major, and E. J. Rouse, "Amputee perception of prosthetic ankle stiffness during locomotion," *Journal of neuroengineering and rehabilitation*, vol. 15, no. 1, p. 99, 2018.

[18] R. L. Waters and S. Mulroy, "The energy expenditure of normal and pathologic gait," *Gait & posture*, vol. 9, no. 3, pp. 207–231, 1999.